Structure of confined adhesive fluids: A Monte Carlo study

A. Jamnik
Department of Chemistry, University of Ljubljana, 61000 Ljubljana, Slovenia

D. Bratko*
College of Chemistry, University of California, Berkeley, California 94720
(Received 17 February 1994)

Canonical and grand canonical Monte Carlo simulations are used to study the structure of Baxter's adhesive fluid [J. Chem. Phys. **49**, 2770 (1968)] in planar slits and its distribution between the pores and the homogeneous phase. The fluid-wall contact densities are determined to calculate the pressure as a function of the density and the separation between the walls. The simulation results are compared with the predictions of the Percus-Yevick approximation for planar pores. A fair agreement between the two methods is found at wider pores and moderate densities and temperatures at which the Percus-Yevick theory conforms with the simulations in the homogeneous phase. In very narrow pores, a truncated graphical expansion provides a better estimate for fluid distribution in the pore.

PACS number(s): 61.20.Ja, 47.55.Mh

I. INTRODUCTION

Understanding the properties of inhomogeneous fluids is fundamental to a variety of problems in colloid science, biophysics, and engineering. Thermodynamic and structural behavior of liquids at interfaces has therefore long been the subject of intense experimental and theoretical research but there remain many important phenomena whose molecular interpretation is still incomplete. Notable examples are the complex phase behavior of confined fluids and the solvent mediated forces among colloids or macroscopic particles in the solution. Neither the long-ranged liophobic interaction [1–4] nor the remarkable properties of liquids in the immediate vicinity of the solid phase [5] have so far been given a plausible microscopic interpretation. While many pertinent questions invite the application of detailed molecular potentials and powerful statistical mechanical methods or simulations, the interest in simpler, analytically tractable models remains alive, and numerous studies of such systems, both analytical and numerical, continue to emerge in the literature. Useful insights into solvation in colloidal systems have been provided by using the models with purely hard-core interactions among the solvent molecules [6–12]. An even better model which combines the analytic tractability with the essential properties of intermolecular potentials such as the packing effects and the short-ranged attractive forces is the Baxter's adhesive fluid [13]. The model treats the molecules as hard spheres with an infinitely deep and infinitesimally short-ranged attractive potential. Analogous adhesion can also be applied to study the wall-particle adsorption [6]. When used in combination with a suitable approximate theory, the adhesive-sphere model displays many characteristic features of real fluids including a reasonable phase behavior in both the pure fluid and in mixtures [14–22]. It has already been proven useful in modeling the interfacial equilibrium [23,24] and the solvation interactions in colloidal solutions [25–29]. These convenient properties are, however, contingent on approximations concealing thermodynamic instabilities of many-body systems with Baxter's potential. As shown by Stell and Williams [30], the successful performance of the Percus-Yevick (PY) [13], the mean spherical (MSA) [31], and related integral equation approximations [32] for sticky hard spheres derives from the neglect of a series of nonintegrable multimolecular clusters which otherwise contribute to the pathological properties of the model. According to these authors [30], the Baxter's approximate solution to the Ornstein-Zernike (OZ) equation is relevant to slightly modified systems with weak polydispersity or with small irregularities in molecular size or shape that do not visibly alter the pair interactions or the properties of smaller molecular clusters but would prevent the formation of large and highly regular critical aggregates conditioned by the perfect geometry and monodispersity of the particles. This puts the approximate PY model in line with typical colloidal and molecular fluids whose pair interactions and small molecular clusters are adequately described by the idealized potential, whereas their microscopic properties do not favor the formation of closely packed aggregates that would correspond to the ignored configurations. The same remarks hold for simulations performed so far with the adhesive model. The simulation techniques described in recent works [33,34] lead to a good agreement with the predictions of the PY sticky sphere model in a broad range of conditions, the results of the two methods being practically indistinguishable at low packing fractions of the fluid. This close correspondence has been achieved by using the Monte Carlo (MC) algorithm that does not sample over the critical clusters also truncated in the Percus-Yevick approximation [30,33–35]. While this does not secure a complete equivalence of the two methods, the properties of the two

*Also affiliated with the J. Stefan Institute, Ljubljana, Slovenia.

model systems appear to be dominated by the terms retained in both approaches. This makes the Monte Carlo method a useful approach to model fluids with the "truncated" Baxter's potential. In the present work, the simulation method of Seaton and Glandt [33] and Kranendonk and Frenkel [34] will be exploited to probe the properties of the adhesive fluid confined in narrow planar pores, possibly in equilibrium with a homogeneous phase, i.e., the system previously considered within the singlet Percus-Yevick–Ornstein-Zernike approximation [28]. The densities and temperatures will be chosen from the range where the results of both methods [13,33,34] nearly coincide in the homogeneous phase. The singlet PY theory is known to become less reliable with increasing degree of confinement [36–38], a deficiency unrelated to the particular choice of the intermolecular potential. The Monte Carlo method free of the approximations of a singlet integral equation theory is therefore used to provide an alternative account of the restricted geometry on the properties of the model fluid. We further note the reduced probability of multimolecular aggregates in the vicinity of the interface. The critical clusters may be sterically excluded from very narrow pores. At these conditions, the present results become independent of the truncations needed in the PY and in the MC treatment of homogeneous or moderately confined Baxter's fluid. The simulation technique of [33,34], here generalized to the restricted geometry and to the implementation of the grand canonical ensemble Monte Carlo (GCMC) simulation, will be applied to study the effects of the stickiness of the fluid on its absorption, the structure in the slit, and the pressure exerted on the walls of the confinement. The details of the model and the simulation are described in Sec. II where a brief outline of the PY equations and of an alternative integral equation approximation for adhesive spheres in narrow slits are also included. The simulation results obtained in the canonical and grand canonical ensemble are collected in Sec. III where the comparisons with selected PY results and with the prediction of the truncated graphical expansion around the narrow pore limit are also made. The performance of analytic theories for inhomogeneous systems is evaluated and future work is briefly discussed.

II. MODEL AND METHODS

A. Percus-Yevick approximation for adhesive spheres

The model used here is identical to that described in our previous article [28]. The sticky-hard-sphere fluid [13] (denoted by 2) is confined between parallel smooth hard plates (1) with the lateral dimensions much bigger than the separation between the walls. The fluid confined in the pore is in equilibrium with a reservoir of bulk fluid at the prescribed number density ρ_b and chemical potential μ. The walls are parallel to the plane $(0,y,z)$ and are located at $x=\pm L/2$. The diameter of the spheres is R, so only the width $L'=L-R$ is available to their centers. The molecules interact among themselves through the square-well potential $\phi_{22}(r)$,

$$\beta\phi_{22}(r)=\begin{cases}+\infty\ , & 0<r<R' \\ -\ln\left|\dfrac{R}{12\tau(R-R')}\right|\ , & R'<r\le R \\ 0\ , & r>R\ ,\end{cases} \tag{1}$$

in the limit $R'\to R$ [13]. This corresponds to an infinitely deep and infinitesimally narrow attractive potential well leading to a finite probability of one particle touching another particle. The Boltzmann factor $\exp[-\beta\phi_{22}]$ in this limit becomes

$$\exp[-\beta\phi_{22}(r)]=\frac{R}{12\tau}\delta(r-R^-)+\Theta(r-R)\ . \tag{2}$$

Above, $\beta=1/kT$, k is the Boltzmann constant, and T the absolute temperature; Θ and δ are the step and the Dirac δ functions, respectively; and τ is the stickiness parameter related to the strength of adhesion and to the temperature of the system [23]. The adhesion strength decays with increasing τ, $\tau=\infty$ corresponding to the absence of attractive interaction.

The wall-fluid hard-core potential is given by

$$\phi_{12}(x)=\infty \quad \text{if } |x|>L'/2 \tag{3}$$

and zero otherwise.

Due to the planar symmetry of the wall-fluid interaction potential, Eq. (3), the average fluid number density in the gap depends only on the perpendicular coordinate x. In the preceding article [28], the distribution of the adhesive spheres in the slit has been estimated within the framework of the Percus-Yevick integral equation theory summarized in the following paragraphs. The Ornstein-Zernike equation for the wall (1)-fluid (2) distribution

$$h_{12}(x)=c_{12}(x)+\rho_b\int h_{13}(|\mathbf{x}-\mathbf{x}'|)c_{23}(\mathbf{x}')d\mathbf{x}' \tag{4}$$

was used along with the Baxter's PY expression for the direct correlation function c_{23} for the adhesive-hard-sphere fluid in the homogeneous phase [13]:

$$c(r)=[-\alpha-\beta r/R-\frac{1}{12}\pi\rho_b\alpha r^3 -\frac{1}{72}\pi\rho_b\lambda^2R^4/r]\Theta(R-r)+\frac{\lambda}{12}\delta(r-R^-)\ , \tag{5}$$

where

$$\alpha=(1+2\eta-\mu)^2/(1-\eta)^4\ ,$$

$$\beta=\frac{-3\eta(2+\eta)^2+2\mu(1+7\eta+\eta^2)-\mu^2(2+\eta)}{2(1-\eta)^4}\ ,$$

and $\mu=\lambda\eta(1-\eta)$. Above, $h_{ij}=g_{ij}-1$ is the total correlation function. λ determines the mean coordination number of molecules. Its value represents the smaller root of the equation [13]

$$\frac{\eta}{12}\lambda^2-\left[\frac{\eta}{1-\eta}+\tau\right]\lambda+\frac{1+\eta/2}{(1-\eta)^2}=0\ , \tag{6}$$

which remains equal as in pure adhesive fluid. According

to the simple form of the wall-fluid model potential, the PY relations for the hard-wall–adhesive-hard-sphere correlations read $c_{12}(x)=0$ at $|x|<L'/2$ and $h_{12}(x)=-1$ if $|x|>L'/2$. The numerical solution of Eq. (4), based on the Picard iteration and the use of the mixing parameter, is described in detail in [28]. In view of the different symmetries of the functions $c(r)$ and $h(x)$ under the integral, the latter was rewritten in the form

$$h(x)=2\pi\rho_b\int_{-1}^{1}h(u+x)S(u)du$$
$$=\int_{-1}^{1}h(u+x)du\,2\pi\rho_b$$
$$\times\int_{0}^{(1-u^2)^{1/2}}c_{\mathrm{PY}}(\sqrt{r'^2+u^2})r'dr' , \qquad (7)$$

where the distances are expressed in units of R. As the function c_{PY}, Eq. (5), is related only to the bulk system, the values of the integral $S(u)$ calculated by the analytic expression

$$S(u)=2\pi\rho_b\{-\alpha(1-u^2)/2-\beta(1-u^3)/3$$
$$-\pi\rho_b\alpha(1-u^5)/60-\pi\rho_b\lambda^2(1-u)/72$$
$$+\lambda/12\} \qquad (8)$$

were tabulated prior to the iteration procedure.

B. Truncated graphical expansion for fluid distribution in narrow pores

Previous studies of hard spheres in confined systems [11,36–38] indicate the PY theory to be reliable only at low to moderate densities and sufficiently wide pores in which the molecule-molecule correlations, approximated by the direct correlation function c_{23} in OZ Eq. (4), remain similar as in the homogeneous phase. For this reason, we also consider an alternative approach to fluid behavior in narrow slits based on the graphical expansion around the known result [11,38,39] for vanishing width of the pores. As in previous works, we begin by considering the classical expression [40]

$\ln(\rho/z)$ = 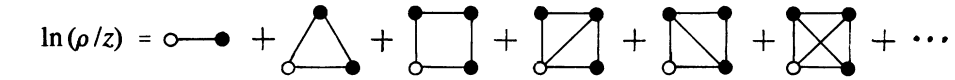 (9)

which relates the local density ρ to the fugacity z of the fluid. As pointed out in [11,38,39,41], the cluster series of Eq. (9) for confined systems converges faster than in the bulk phase [11]. The contribution of many-particle terms to the above series decreases with the degree of confinement of the fluid. In earlier studies of confined fluid with purely hard-core interaction, we found [11,38] the leading, two-particle term in the series of Eq. (9) to be quite sufficient at low reduced densities $\rho_b R^3<0.3$ and the slit width below $1.5R$. At higher bulk densities, the validity of this approximation was restricted to smaller wall-wall separations. The addition of the short-ranged sticky potential does not appear to reduce the deficiencies of the singlet theories applied to narrow confinement. For small separations between the walls L, it is therefore interesting to examine the truncated form of Eq. (9):

$\ln(\rho/z) \approx$ 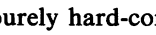 (10)

earlier termed the B_2 approximation [38]. With sufficiently short-ranged potentials, all integrals in Eq. (9) vanish at $L\to R$, giving the exact limiting relation [11,38,39,41]

$$\rho\to z \quad \text{when } L\to R,\ L'\to 0 . \qquad (11)$$

Equation (10) represents the first order correction beyond this limiting result. The fluid fugacity $z=\rho_b\exp(\beta\mu_b')$ and μ_b' is the excess chemical potential of the bulk fluid. Its dependence on the density of the fluid can be obtained either by grand canonical Monte Carlo simulation of the bulk phase or from the extrapolation of GCMC's densities in sufficiently narrow pores to $L=R$. The simulation procedures are described in Sec. II C. In analytic calculations, we determine the fugacity by using the PY compressibility pressure equation [13]

$$\frac{\beta P}{\rho_b}=\frac{1+\eta+\eta^2-\mu(1+\eta/2)+\eta^{-1}\mu^3/36}{(1-\eta)^3} . \qquad (12)$$

We begin from the thermodynamic relation

$$d\ln z=\frac{\beta}{\rho_b(P)}dP \qquad (13)$$

and obtain z by integrating both sides of Eq. (13) over the range $[z_{\mathrm{low}},z]$ and $[\beta P_{\mathrm{low}},\beta P]$, where the upper limit represents the reduced pressure from Eq. (12) for the bulk density of our interest. For the lower limit, a finite but sufficiently small value of the density has to be taken to ascertain the limiting equality, $z\to\rho$ when $\rho\to 0$. The discrete points of the integrand for the numerical integration in the final expression,

$$z=\beta P_{\mathrm{low}}\exp\left\{\int_{\beta P_{\mathrm{low}}}^{\beta P}d(\beta P)/\rho_b(\beta P)\right\} , \qquad (14)$$

are obtained by iteration of Eq. (12). A density profile of the adhesive-hard-sphere fluid in a narrow gap can now be obtained from Eq. (10), rewritten as

$$\ln\frac{\rho(\mathbf{r}')}{z}=\int f(\mathbf{s})\rho(|\mathbf{r}'-\mathbf{s}|)ds \ . \tag{15}$$

Here, f is the Mayer function,

$$f(r)=\exp[-\beta\phi(r)]-1 \ .$$

In the case of the adhesive potential, it takes the form

$$f(r)=\begin{cases}-1+\dfrac{1}{12\tau}\delta(r-1^-) \ , & r\le 1\\ 0 \ , & r>1 \ .\end{cases} \tag{16}$$

The resulting integral equation for $\rho(x)$ is

$$\ln\frac{\rho(x)}{z}=-\pi\int_{x-1}^{x+1}\rho(x')\left\{[1-(x-x')^2]-\frac{1}{6\tau}\right\}dx' \ , \tag{17}$$

where the opposite contributions of the excluded volume of the molecules [11] and of their surface adhesion are reflected in terms included in the integrand. The integral in Eq. (17) was solved in a similar way as the PY-OZ equation (7).

C. Simulation

The adhesive potential described in Eqs. (1) and (2) implies finite probabilities of contact configurations between molecular pairs. This property is related to the infinite depth of contact intermolecular potential, a feature which cannot be captured by the conventional Monte Carlo method with particles moving at random in a three-dimensional space. The problem can be overcome by monitoring the particle motion in a transformed configurational space where finite volumes are being assigned to the energetically favored binding configurations. The subvolumes corresponding to specific binding states represent a direct measure of their probability. The integration of the Boltzmann factor, Eq. (2), across the surface comprising the contact configurations for two particles results in the single-bond subvolume, and double or triple integration across the line comprising the double-bond states, or the point where a triple bond is possible, will have a similar effect. This idea has been exploited in simulation studies of homogeneous adhesive fluid carried out by Seaton and Glandt [33] and Kranendonk and Frenkel [34]. In these works, no provisions have been made to consider explicitly the possibility of the quadruple or higher order coordination. As noted in the Introduction, this technique does not provide exact results for the original Baxter's model but rather for a system with a somewhat modified Hamiltonian devoid of the highly packed critical aggregates and of the concomitant thermodynamic instabilities [30,35]. Its results have been found to be in good agreement with the adhesive model in the PY approximation. The present work is concerned with the behavior of this model at interfaces and planar confinement, the simulation being used to study the effect of spatial constraint under the conditions where the PY theory and the Monte Carlo method agree in the isotropic phase. While the MC algorithms of [33] and [34] appear essentially equivalent, the method of the latter authors proved more flexible regarding to optimization of the acceptance of the simulation moves. This algorithm has therefore been adopted in our work. The effects of the confinement were studied by introducing geometrical restrictions along a chosen direction. In the following paragraphs, we describe this modification together with the main features of the basic Kranendonk-Frenkel method, a detailed description of which is to be found in their original paper [34]. After that, we introduce an algorithm for open ensemble simulation designed to study the partitioning of the adhesive fluid between the homogeneous phase and the porous material.

1. Canonical simulation

If we identify the adhesive interaction by a formation of a bond between a pair of molecules, a trial step in the Kranendonk-Frenkel MC method consists of an attempted displacement of a particle at a fixed number of bonds or of an attempt to change the number of bonds. The simulation may begin by placing N unbounded particles at randomly chosen nonoverlapping configuration. Then, in each step, an attempt is made to move a randomly chosen particle to a random position within the so-called test sphere [34] whose radius is equal to the displacement parameter adjusted according to the density of the fluid. During the actual displacement of a b-times bonded particle, its number of bonds may change from b to b', b and b' ranging from 0 to 3, the restriction initially introduced to enhance the efficiency of the method. As discussed in [30] and in the preceding paragraphs, this limitation has profound consequences, since it effectively prevents the sampling over the class of critical aggregates and suppresses the instabilities of the model in a similar way as do the truncations introduced in approximate integral equation theory [30,35].

Each move involving zero to triple bonded states corresponds to a displacement in three to zero actual dimensions or, alternatively, to a move within the three-dimensional subvolumes of the rescaled configurational phase space in which the volume elements are expanded in proportion to the Boltzmann factors of a specified configuration. In this space, the so-called effective volumes of each particular degree of binding, covering all the realizations of given type of bond b inside the test sphere, are defined [34] by the expression

$$V_{\text{eff}}(b)=\sum_i\left[\frac{R}{12\tau}\right]^b\int dq_i \ . \tag{18}$$

dq_i represents all degrees of freedom, remaining after the formation of the bond(s). A particular configuration is then selected with the probability

$$P(i)=\frac{V_{\text{eff}}^{(i)}}{\sum_{i=0}^{3}V_{\text{eff}}^{(i)}} \ , \tag{19}$$

its magnitude obviously depending on the local structure

in the test sphere. A new configuration is automatically accepted unless a hard-core overlap has been detected. In restricted geometry, the rejection applies to the moves leading to an overlap of the moved particle with another molecule or with the boundaries of the confinement. The simplest and quite usual geometry considered in theoretical studies of confined fluids is the one of a planar slit consisting of two parallel, perfectly smooth hard walls at a specified separation L. Denoting the perpendicular direction by x, the fluid between the walls extends to infinity along the directions y and z, parallel to the walls. In practical simulations, the system is modeled as an infinite array of identical simulation cells of the volume $L\times a^2$, repeating themselves in the two lateral directions. When dealing with a fluid with short-ranged interactions, such as those of our present interest, this amounts to the application of the minimum image convention along the directions y and z. No periodicity needs to be assumed in the direction x normal to the plates. Canonical Monte Carlo simulation (CMC) in this kind of a system allows us to study the effect of the constraints on the structure of a fixed amount of the fluid within the pore. More interesting cases involve the equilibrium between the fluid in the pore and the homogeneous bulk phase. The constant fugacity and not the number of the particles should be used as the input information in modeling of this kind of system. The grand canonical ensemble MC method will therefore be introduced shortly. The computationally less demanding CMC technique is, nevertheless, a useful tool in several situations, including the studies of closed systems and the modeling of wide pores where there exist domains of the fluid sufficiently distant from both walls to retain practically nonperturbed density and other properties of the bulk phase. As the mean number of particles in a GCMC converges more rapidly than does the detailed density profile in the system, the CMC technique can also be combined with the preceding GCMC run in first determining the equilibrium amount and then the structure of the fluid in the pore.

2. *Open ensemble simulation*

In the open ensemble, the number of particles is allowed to fluctuate, the thermodynamic state being defined by constant volume V, temperature T, and the chemical potential of the fluid μ. In this case, the phase space is sampled by the movement of randomly chosen particles (CMC step), and by the addition to or removal of particles from the system (GCMC step). Additions and removals are attempted randomly with a probability P, so the probability of the CMC step is $1-2P$. The value $P\approx 0.15$ was used in most of our runs.

Each addition of a particle may be accompanied by the formation, and similarly, a removal of a particle by the breaking of the bond(s). As has been noted in the context of canonical Monte Carlo simulation, the infinite energy changes accompanying the formation or breaking of the bonds have to be considered in a nonconventional manner. The standard GCMC relations for the acceptance probability of an attempted addition f_{ij} or of a deletion f_{ji}, where $N_j=N_i+1$ [42]:

$$\begin{aligned} &f_{ij}=r\ ,\quad f_{ji}=1\ \text{ if } r\le 1\\ &f_{ij}=1\ ,\quad f_{ji}=\frac{1}{r}\ \text{ if } r>1\ , \end{aligned} \tag{20}$$

with

$$r=\frac{\langle\rho_b\rangle}{\rho_j}\exp[\beta(\mu_b'-u_j+u_i)]\ , \tag{21}$$

have to be suitably modified. Above, $\langle\rho_b\rangle$ and μ_b' are the mean number density and excess chemical potential of the bulk phase, and u_j-u_i is the energy change due to the addition or deletion of a particle. The densities in Eq. (21) have to be replaced by the corresponding expressions for the densities in the rescaled configurational space where zero-, one-, or two-dimensional subvolumes in real space, available to a particle forming three, two, or a single bond are expanded by the Boltzmann's factors:

$$r=\frac{\left\langle\left[N\Big/\sum_{k=0}^{3}V_{\text{eff}}^{(k)}\right]_b\right\rangle}{N_j\Big/\sum_{k=0}^{3}V_{\text{eff}}^{(k)}}\exp[\beta\mu_b'-\Delta u_{ij}]\ . \tag{22}$$

As in Eq. (18), the effective volumes V_{eff} represent independent subvolumes for the specified binding states of the particle. The excess chemical potential has to be determined from an independent GCMC simulation of the bulk fluid prior to studying the inhomogeneous phase. Unlike the CMC simulation, where the calculation of the effective volumes V_{eff} is restricted to the interior of a suitably chosen test sphere, the numerator in Eq. (22) should, in principle, be determined by calculating the effective volumes for the entire MC cell at each GCMC step. This would, of course, consume a prodigious amount of computer time, especially at high densities where the number of available binding configurations may be extremely large. For this reason, we prefer to add and remove only the nonassociated particles and let the number of bonds adjust through internal equilibration during the CMC steps. This leads to a considerable simplification of Eq. (22) where we keep only the terms $k=0$, $\Delta u_{ij}=0$, and $V_{\text{eff}}^{(0)}=V^0=V$. The result

$$r=\frac{\langle\rho_b^0\rangle}{\rho_j^0}\exp[\beta\mu_b^{0\prime}] \tag{23}$$

is quite similar to that of the standard method, Eq. (21), the only difference being in considering only a fraction of the entire number of particles, the nonbounded particles, denoted by the indexes 0. Considering the chemical potential, as well as the standard state of nonbounded particles to be equal to that of the whole system, the following expression for the new parameter B, which is kept constant during the simulation, is obtained:

$$B=\beta\mu_b'+\ln\langle\rho_b\rangle=\beta\mu_b^{0\prime}+\ln\langle\rho_b^0\rangle\ . \tag{24}$$

From its value and the average densities resulting from the simulation, the excess chemical potentials of the fluid and the corresponding value for the nonbounded particles can be determined. The same value of B can then be

used in the simulation of the confined fluid to study the partitioning between the pore and the homogeneous phase. As in the CMC simulations, the density profiles are determined from the average numbers of the particles found within the slices into which the elementary cell is subdivided [8]. The wall-fluid contact number density ρ_{in}^{c} which, in the case of fluid interacting with the wall through the hard-core potential, Eq. (3), determines the pressure on the inner side of the plate, is estimated by extrapolation [11,38,39]. A typical duration of a CMC run was about 20 000 trial moves per particle in the production calculation, and 10 000 moves per particle were needed to equilibrate the system. A GCMC run of a comparable system demanded 30–50 % more configurations. On an IBM RISC 6000/320 workstation, a typical run on a 100- particle system required about 1 h of computer time.

III. RESULTS AND DISCUSSION

The Monte Carlo algorithm for adhesive hard spheres [33,34], here adapted to inhomogeneous systems, is not classified among standard routines of molecular simulation. The programs we have developed by extending the work of Kranendonk and Frenkel [34] were therefore carefully checked against the known results for isotropic systems [33,34]. The distribution functions and related structural quantities [34] were reproduced within the whole range of the density and the reduced temperature considered in the above studies [33,34]. For reasons discussed in Secs. I and II, our simulations of confined systems were carried out at the conditions characterized by good agreement between the properties of simulated homogeneous fluid and the predictions of the Percus-Yevick approximation. For illustration, a set of average coordination numbers c_n of adhesive spheres in homogeneous systems at various densities $\rho_b R^3$ and stickiness parameters τ from these simulations are compared with the Percus-Yevick result, $c_n = 2\lambda\eta$ [18]. The results obtained by the two methods and collected in Table I are in good agreement with each other even at pretty severe conditions $\tau = 0.2$ and $\rho_b R^3 = 0.6$. Within the above range, the simulation is believed to provide an accurate account of steric constraints to be considered in the following examples. In view of technical difficulties encountered in the simulation of the near-glassy states observed at temperatures closer to the critical stickiness $\tau_c = (2-\sqrt{2})/6$ [13], the systems with τ below 0.2 will not be considered in the present work. A detailed PY study of the confined adhesive fluid around and below the critical temperature has been carried out in the preceding work [28].

TABLE I. Average PY [18] and MC coordination numbers c_n of adhesive spheres in homogeneous systems at various densities $\rho_b R^3$ and stickiness parameter τ.

$\rho_b R^3$	τ	c_n (MC)	c_n (PY)
0.2	0.2	0.94	1.00
	0.5	0.44	0.46
	1.0	0.24	0.25
0.4	0.2	1.91	1.92
	0.5	0.98	1.03
	1.0	0.58	0.60
0.6	0.2	2.94	2.87
	0.5	1.71	1.75
	1.0	1.07	1.09

In Fig. 1 we present the CMC and PY single-wall density profiles in the gap of width $L = 4R$ or $L' = 3R$ at different values of bulk density $\rho_b R^3$ and stickiness parameter τ. The bulk density $\rho_b R^3$ enters the calculations through the direct correlation function $c(r)$, Eq. (5), while we used the PY average density in the pore as the input in the CMC simulation. The present results therefore provide a comparison between the Percus-Yevick and the Monte Carlo structures of the confined sticky fluid at fixed mean density in the slit. Judging from PY performance in hard sphere fluids [37,38,43–48] and from the comparisons with the GCMC results for the adhesive molecules to be presented later in this work, the PY estimate of the equilibrium density inside the pore is rather accurate at the pore width considered in the present examples.

Figures 1(a)–1(c) successively illustrate the effect of the increasing attraction among the molecules at bulk densities $\rho_b R^3 = 0.2$, 0.4, and 0.6. The value $\tau = \infty$ corresponds to infinite temperature and hard sphere behavior, while $\tau = 0.2$ describes a gas with strong attractive interactions. The oscillating density profiles revealing the existence of molecular layers parallel to the walls are observed in both the PY theory and in the simulation. The agreement between the two methods is especially good at lower densities and weaker stickiness of the molecules. In systems dominated by hard-core repulsions, the PY theory is known to underestimate the fluid density in the immediate vicinity of the walls [38,49] and the same trend is observed in present calculations at weak adhesion. At low values of τ, corresponding to strong attractive forces among the molecules, the underestimate of intermolecular correlations leads to the opposite result, the PY theory predicting higher contact densities than seen in the simulation. A relatively good agreement observed at the intermediate stickiness of about $\tau = 0.5$ appears to reflect a fortuitous cancellation of the two opposite effects. Both methods reveal the singularities in the profiles $\rho(x)$ at the distance $x = L'/2 - R$ corresponding to the thickness of a monolayer of the fluid adjacent to the wall. The heights of the peak located at this distance coincide within the numerical accuracy of the calculations. Strictly speaking, the simulation results correspond to a Hamiltonian slightly different from the one considered in the PY-OZ approximation. The above comparisons are, however, still useful in assessing the accuracy of the latter method in inhomogeneous systems [28] where the same simulation technique that leads to good agreement with the PY theory in isotropic fluid applies without making any additional approximation. At high temperature τ, both methods predict an accumulation of the molecules next to the walls. In the hard sphere limit, where the simulation is also formally exact, the PY approximation underestimates the contact density

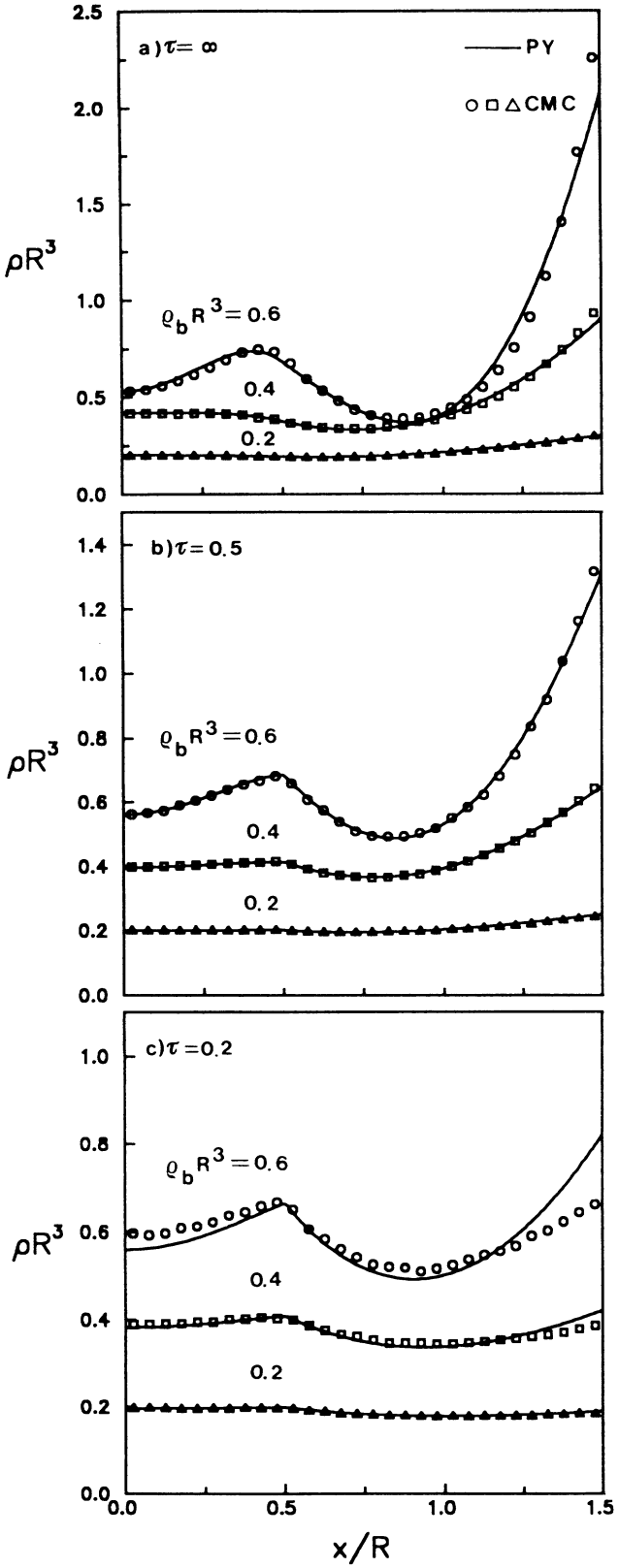

FIG. 1. The PY (lines) and the CMC (symbols) density profiles of the adhesive-hard-sphere fluid in the gap of width $L=4R$ at the values of stickiness parameter (a) $\tau=\infty$ (hard-sphere fluid), (b) $\tau=0.5$, and (c) $\tau=0.2$, at different bulk densities $\rho_b R^3$.

of the fluid at the wall. Upon lowering τ, the tendency of the molecules towards association begins to compete with steric effects. The molecules can only attain a full coordination outside the gap or at sufficient distances from the walls. This leads to lower values of the distribution coefficient K [37,38], defined as the ratio between the average densities in the pore and in the bulk fluid. For not too narrow pores, the PY theory is known to provide a fair estimate of fluid adsorption for systems dominated by repulsive interactions [36–39]. According to the present results, the accuracy of the singlet PY approximation decays with the increasing role of intermolecular attraction. At the strongest adhesion considered in the present calculations, $\tau=0.2$, the densities obtained by both methods differ not only in the vicinity of the walls but nearly everywhere in the gap. The disagreement is most pronounced at the fluid-wall contact plane but affects the profile over the whole width of the pore. The errors in the PY results in the two extreme cases, dominated either by the repulsive or by the attractive interactions among the molecules, are of the opposite sign. The best agreement is, therefore, observed at moderate adhesion, as seen in systems with $\tau=0.5$ where the theory and the simulation conform at all positions in the pore.

Figure 2 represents the situations similar to that of Fig. 1 but for wider gap of $L=7R$ or $L'=6R$, where the structure of the fluid near a single wall is not visibly affected by the presence of the opposite wall. According to both methods used in these calculations, the flat density profiles $\rho(x)=\rho_b$ are restored around the midplane $(0,y,z)$. The present results should therefore be almost identical to the fluid profiles next to isolated walls or walls at infinite separation. The differences between the MC and the PY results observed in the vicinity of the walls are supposed to reflect the approximations of the singlet PY theory, as noted in the discussion of Fig. 1.

Kranendonk and Frenkel applied the constant-pressure simulations to study the phase diagram of the sticky fluid [34]. The calculated pressure vs density dependence was in good agreement with the predictions of the compressibility and the energy equations in the PY approximation. In the present work, we explore an alternative calculation based on the contact theorem that relates the pressure to the wall-fluid contact density according to the equation

$$P_b=\rho^c kT \ . \tag{25}$$

Above, ρ^c is the density of the fluid at the surface of the hard wall of the container or the gap sufficiently wide to eliminate the effect of the size on the wall-fluid distribution. In narrow pores with overlapping density profiles, the contact density at the walls and the concomitant force per unit area depend on the distance between the walls. In the case of parallel plates immersed in the fluid, this gives rise to the distance dependence of the solvation force F, proportional to the difference between the pressures exerted by the fluid molecules on the inner and the outer side of the plates, $F/S=[\rho^c_{\text{in}}-\rho^c_{\text{out}}]kT$. The inner contact density ρ^c_{in} approaches the outer value corresponding to the bulk pressure of the fluid with increasing

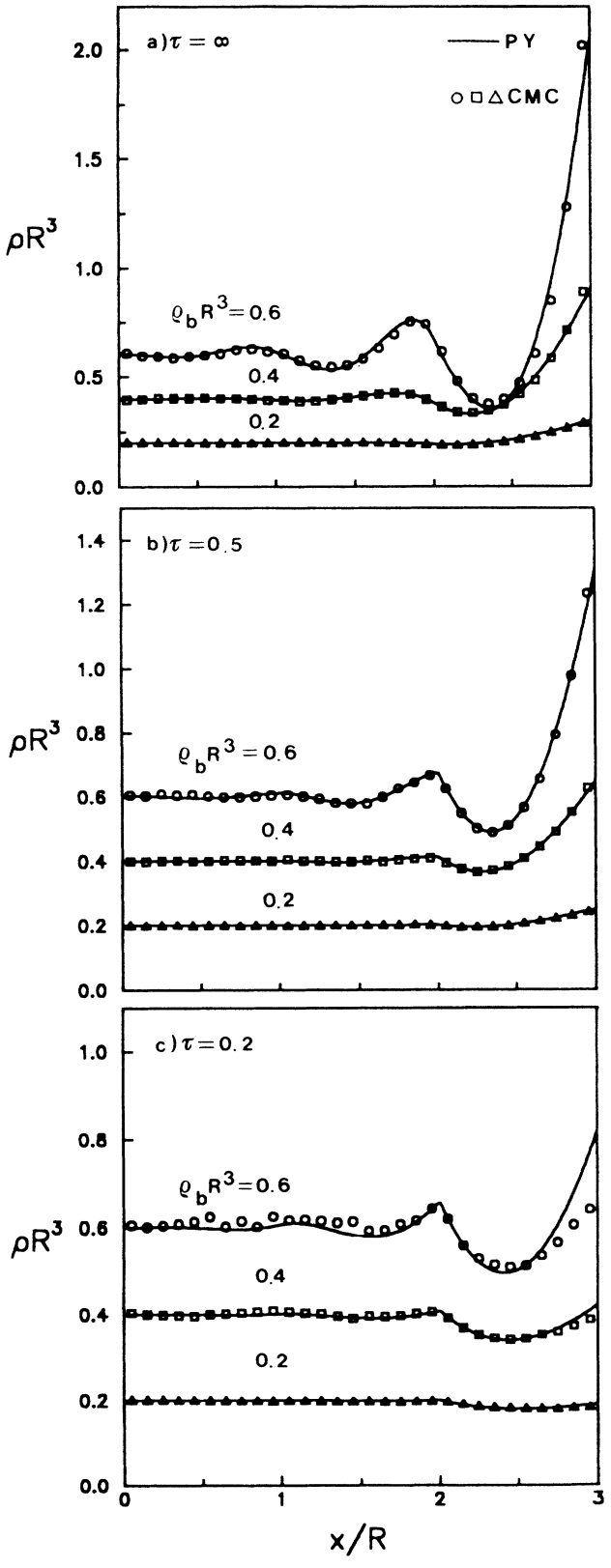

FIG. 2. The PY and the CMC density profiles of the adhesive-hard-sphere fluid in the gap of width $L=7R$ at the values of stickiness parameter (a) $\tau=\infty$, (b) $\tau=0.5$, and (c) $\tau=0.2$ at different bulk densities $\rho_b R^3$.

separation between the walls. The inner pressure $\rho_{in}^c kT$ obtains the value of the bulk pressure at separations sufficient for the fluid around the midplane of the gap to remain nonperturbed by the presence of the walls. In Fig. 3 we present the isotherms P vs ρ_b obtained from the CMC wall-fluid contact densities in the pore with $L=11R$, a width more than sufficient to fulfill the above condition. The calculated CMC pressures are in complete agreement with the results of more demanding isobaric simulations collected in Fig. 2 of [34]. As pointed out in the latter work, the simulation pressures are also quite close to the predictions of the Percus-Yevick approximation combined with the compressibility equation. In view of the exact relation (25), the consistency of the present results with those obtained in the isobaric simulations [34] confirms the accuracy of given simulation technique in calculations of the fluid distribution in inhomogeneous systems.

The fluid structure in wide pores such as those considered in Figs. 1–3 can be described fairly accurately within the singlet PY approximation [28]. In narrower gaps, where the correlations among the molecules are appreciably different from those in the homogeneous phase, the singlet theory becomes less reliable. These conditions invite the application of an alternative analytic approximation, the truncated graphical expansion, earlier termed the B_2 approximation [38]. According to Eqs. (9) and (10), this approximation is effectively an expansion of the density profile around the exact narrow pore limit given by Eq. (11). In practical application, its reliability rests on accurate input fugacity corresponding to the bulk phase in equilibrium with the confinement. The fugacity can readily be obtained from the pressure-density dependence determined by applying the PY theory to the homogeneous phase. In Table II the calculated fugacities

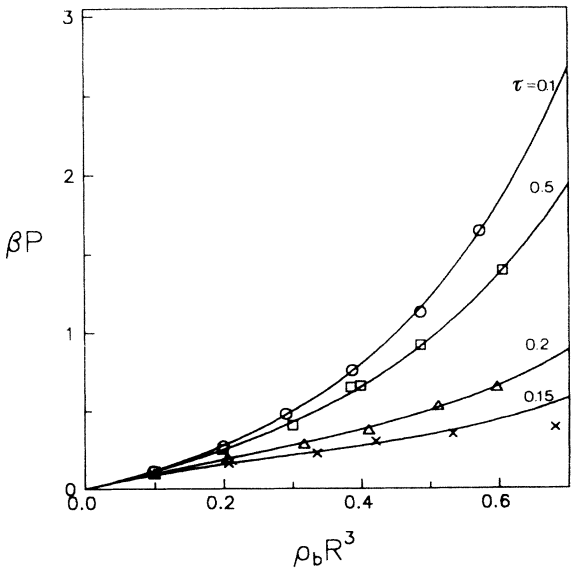

FIG. 3. The density dependence of the pressure of the adhesive fluid determined by the PY compressibility equation (lines) and from the CMC simulations of the confined system in the gap of the width $L=11R$ (symbols) at different effective temperatures τ.

TABLE II. The fugacities z and the reduced excess chemical potentials $\beta\mu_b'$ determined by (a) using the Baxter's equation of state of the adhesive fluid, Eqs. (12)–(14); (b) GCMC simulations of the homogeneous system; and (c) the limiting GCMC densities in vanishingly narrow pores, at various bulk densities $\rho_b R^3$ and stickiness parameters τ.

		$\beta\mu_b'$			Fugacity		
$\langle\rho_b R^3\rangle$	τ	(a)	(b)	(c)	(a)	(b)	(c)
0.230	0.2	−0.168	−0.131	−0.130	0.195	0.202	0.202
0.406		−0.177	−0.160	−0.160	0.341	0.346	0.346
0.648		0.062	−0.066	−0.065	0.689	0.607	0.607
0.214	0.5	0.527	0.542	0.540	0.363	0.368	0.367
0.416		1.235	1.277	1.278	1.431	1.492	1.494
0.600		2.182	2.261	2.263	5.318	5.754	5.765

z and the reduced excess chemical potentials $\beta\mu_b' = \ln(z/\rho_b)$ calculated by Eqs. (12)–(14) are compared with the grand canonical Monte Carlo results at different bulk densities $\rho_b R^3$ and the stickiness parameters τ. The densities are the statistical averages obtained in GCMC simulations of bulk systems at specified values of the excess chemical potential μ_b'. The fugacities and excess potentials in the first column (a) are obtained by integration of Baxter's analytical equation of state, Eqs. (12)–(14); the second column (b) contains the GCMC results for the bulk phase. The third column (c) lists the limiting GCMC densities in vanishingly narrow pores, determined by extrapolation of the mean pore density to the pore width $L = R$. Since Eq. (11) is exact, the slight differences between the two GCMC results represent merely a measure of the statistical uncertainty of the simulation procedures. It may also be noted that the spatial constraints encountered in simulations in narrow slits eliminate the critical clusters [30] leading to the instability of the fluid with the original Baxter's Hamiltonian. The connection with the truncated Hamiltonian implied in the given Monte Carlo procedure [33,34] is, however, retained through assumed equilibrium with the homogeneous phase. The comparison between the MC and the PY data, on the other hand, reveals a fair agreement between the two approaches, the PY theory doing a better job at weaker stickiness and lower densities of the fluid.

According to Figs. 1 and 2, the CMC and the PY approximation are in a fair agreement when L is large enough. The difference is most pronounced at the fluid-wall contact plane, the deviation of the contact densities ρ^c is therefore the most suitable measure for the comparison between the two methods. For this reason, and also because ρ^c determines the pressure exerted on the wall of the gap and, consequently, the solvation force between the walls, we now present the results of the GCMC, PY, and B_2 approximations for ρ^c as a function of the gap width L. In Fig. 4 the results for $\tau=0.2$ and 0.5, and $\rho_b R^3=0.648$ and 0.600, i.e., the highest densities from Table II, are collected. The comparison among the three approaches is similar to that found earlier in systems with purely repulsive interactions [11,38]. The PY theory is relatively successful in wider pores, while the B_2 approximation is applicable only in narrow slits of the

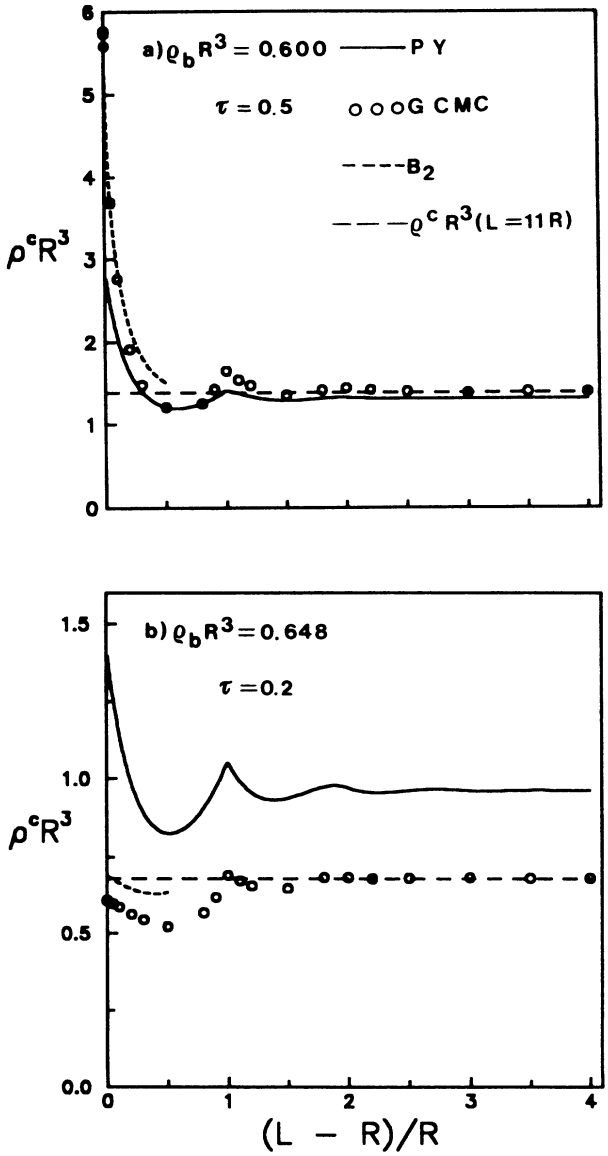

FIG. 4. The PY, GCMC, and B_2 wall contact density $\rho^c R^3$ as a function of the gap width at (a) the bulk density $\rho_b R^3=0.600$ and the value of the stickiness parameter $\tau=0.5$ or (b) $\rho_b R^3=0.648$ and $\tau=0.2$.

width barely exceeding the diameter of the molecules. The overall accuracy of either approximate method decreases with the density of the bulk phase, although the B_2 results remain exact in extremely narrow pores at any concentration. For weaker attractive interactions among the molecules corresponding to $\tau=0.5$, both theories are satisfactory, the B_2 approximation for small L' being in an almost quantitative agreement with the GCMC results. Only the range $L' \leq 0.5R$ is considered in B_2 calculations since higher terms of cluster expansion, Eq. (9), become increasingly important in wider slits. The agreement between the GCMC and the B_2 approximation is worsened at lower temperature or stronger attraction among the molecules, when the PY estimate of the excess chemical potential represents a somewhat poorer approximation. At the same time, only a qualitative agreement between the singlet PY theory and the GCMC results is retained at the temperature $\tau=0.2$. The calculated solvation force between the plates immersed in the fluid reveals even bigger differences between the two methods. The force per unit area is proportional to the difference between the contact densities at the given wall-wall separation and the corresponding wide pore limit to which ρ^c converges with increasing L. Figure 4(b) shows the PY solvation force to oscillate between attraction and repulsion, while the simulation at a given stickiness reveals predominantly attractive interaction at all separations between the plates.

These comparisons have, of course, a somewhat different meaning than usually presumed in parallel theoretical and simulation studies. The simulation technique adopted in the present study does not provide exact results for the original sticky-sphere model [13] but corresponds to a slightly different Hamiltonian in which one neglects an infinite series of highly coordinated critical configurations [30] in a manner similar to that of the PY approximation for intermolecular correlations. The applied MC method has been proved to conform with the PY theory in homogeneous solutions. Unlike the latter, however, it applies to inhomogeneous systems without invoking additional approximations and treats the confined fluid at precisely the same level of accuracy as does the bulk phase. The applicability of the analytic theory to systems of restricted geometry is therefore assessed in the conventional manner. There is, however, additional motivation for the development of simulation techniques for fluids with Baxter's potential. As pointed out in earlier works [39,50–52], the introduction of orientation dependence of intermolecular adhesion opens a promising route for modeling of molecular fluids with nonspherical pair potentials. While retaining the advantages of analytic tractability, these systems may, upon a suitable choice of model parameters, be free of reservations applying to the original Baxter's model [30]. Extensions of the present simulations to fluids with anisotropic adhesion are therefore planned along with integral equation studies of homogeneous and nonhomogeneous fluids with multipolar adhesive interaction.

ACKNOWLEDGMENTS

The authors thank Professor D. Henderson, Professor L. Blum, Professor E. Y. Chiew, and Professor E. D. Glandt for their comments and helpful discussions.

[1] J. N. Israelachvili, *Intermolecular and Surface Forces* (Academic, London, 1985).
[2] R. G. Horn and B. W. Ninham (unpublished); *Micellar Solutions and Microemulsions: Structure, Dynamics and Statistical Thermodynamics,* edited by S. H. Chen and R. Rajagopalan (Springer, New York, 1990), p. 81.
[3] J. R. Grigera, L. Blum, and H. E. Stanley (unpublished).
[4] Y. H. Tsao, D. F. Evans, and H. Wennerström, Science **262**, 547 (1993).
[5] S. Granick, Science **253**, 1374 (1991); **258**, 1339 (1992).
[6] A. J. Post and E. D. Glandt, J. Colloid Interface Sci. **108**, 31 (1985).
[7] D. Henderson, Fluid Phase Equil. **76**, 1 (1992).
[8] G. Karlström, Chem. Scr. **25**, 85 (1985).
[9] Y. Zhou and G. Stell, Mol. Phys. **66**, 767 (1989).
[10] D. Henderson, J. Colloid Interface Sci. **121**, 486 (1988).
[11] M. S. Wertheim, L. Blum, and D. Bratko (unpublished); *Micelles and Microemulsions: Structure, Dynamics and Statistical Thermodynamics,* edited by S. H. Chen and R. Rajagopalan (Springer, New York, 1990), p. 99.
[12] T. Biben and J. P. Hansen, Europhys. Lett. **V12**, 347 (1990).
[13] R. J. Baxter, J. Chem. Phys. **49**, 2770 (1968).
[14] R. O. Watts, D. Henderson, and R. J. Baxter, Adv. Chem. Phys. **21**, 421 (1971).
[15] B. Barboy, J. Chem. Phys. **61**, 3194 (1974).
[16] B. Barboy, Chem. Phys. **11**, 357 (1975).
[17] S. Smithline and A. D. J. Haymet, J. Chem. Phys. **83**, 4103 (1985).
[18] Y. C. Chiew and E. D. Glandt, J. Phys. A **16**, 2599 (1983).
[19] D. Y. C. Chan, B. A. Pailthorpe, J. S. McGaskill, P. J. Mitchell, and B. W. Ninham, J. Colloid Interface Sci. **72**, 27 (1979).
[20] N. A. Seaton and E. D. Glandt, J. Chem. Phys. **87**, 1785 (1987).
[21] C. F. Tejero and M. Baus, Phys. Rev. E **48**, 3793 (1993).
[22] M. Banaszak, Y. C. Chiew, and M. Radosz, Phys. Rev. E **48**, 3760 (1993).
[23] P. T. Cummings, J. W. Perram, and E. R. Smith, Mol. Phys. **31**, 535 (1976).
[24] D. W. Marr and A. P. Gast, J. Chem. Phys. **99**, 2024 (1993).
[25] A. Jamnik, D. Bratko, and D. Henderson, J. Chem. Phys. **94**, 8210 (1991).
[26] M. H. G. M. Penders and A. Vrij, Physica A **173**, 532 (1991).
[27] A. Jamnik and D. Bratko, Vestn. Slov. Kem. Drus. **38**, 39 (1991).
[28] A. Jamnik and D. Bratko, Chem. Phys. Lett. **203**, 465 (1993).
[29] M. H. G. M. Penders and A. Vrij, Prog. Colloid. Polym. Sci. **89**, 1 (1992).

[30] G. Stell, J. Stat. Phys. **63**, 1203 (1991); G. Stell and G. O. Williams (unpublished).
[31] J. J. Brey, A. Santos, and F. Castano, Mol. Phys. **60**, 113 (1987); L. Mier y Teran, E. Corvera, and A. E. Gonzales, Phys. Rev. A **39**, 371 (1989).
[32] S. B. Yuste and A. Santos, Phys. Rev. E **48**, 4599 (1993).
[33] N. A. Seaton and E. D. Glandt, J. Chem. Phys. **84**, 4595 (1986).
[34] W. G. T. Kranendonk and D. Frenkel, Mol. Phys. **64**, 403 (1988).
[35] E. D. Glandt (personal communication).
[36] E. D. Glandt, J. Colloid Interface Sci. **77**, 512 (1980).
[37] E. D. Glandt, AIChE J. **27**, 51 (1981).
[38] D. Bratko, L. Blum, and M. S. Wertheim, J. Chem. Phys. **90**, 2752 (1989).
[39] A. Luzar, D. Bratko, and L. Blum, J. Chem. Phys. **86**, 2955 (1987).
[40] H. L. Friedman, *A Course in Statistical Mechanics* (Prentice Hall, Engelwood Cliffs, New Jersey, 1985).
[41] D. Bratko, D. Henderson, and L. Blum, Phys. Rev. A **44**, 8235 (1991).
[42] J. P. Valleau and G. M. Torrie, in *Statistical Mechanics,* edited by B. J. Berne (Plenum, New York, 1977), Part A, p. 169.
[43] J. M. D. MacElroy and S. H. Suh, AIChE Symp. Ser. **82**, 133 (1986).
[44] S. H. Suh and M. D. MacElroy, Mol. Phys. **58**, 445 (1986).
[45] J. M. D. MacElroy and S. H. Suh, Mol. Phys. **60**, 475 (1986).
[46] Y. Zhou and G. Stell, J. Chem. Phys. **89**, 3836 (1988).
[47] Y. Zhou and G. Stell, J. Chem. Phys. **89**, 7020 (1988).
[48] Y. Zhou and G. Stell, J. Chem. Phys. **91**, 3208 (1989).
[49] D. Nicholson and N. G. Parsonage, *Computer Simulation and the Statistical Mechanics of Adsorption* (Academic, London, 1982).
[50] D. Bratko, L. Blum, and A. Luzar, J. Chem. Phys. **83**, 6367 (1985).
[51] P. T. Cummings and L. Blum, J. Chem. Phys. **84**, 1833 (1986).
[52] L. Blum, P. T. Cummings, and D. Bratko, J. Chem. Phys. **92**, 3741 (1990).